

University of Groningen

## SHG FROG characterization of

Baltuška, Andrius; Pshenichnikov, Maxim S.; Wiersma, Douwe A.

*Published in:*

Technical Digest. Summaries of papers presented at the Conference on Lasers and Electro-Optics, 1998. CLEO 98

**IMPORTANT NOTE: You are advised to consult the publisher's version (publisher's PDF) if you wish to cite from it. Please check the document version below.**

*Document Version*

Publisher's PDF, also known as Version of record

*Publication date:*

1998

[Link to publication in University of Groningen/UMCG research database](#)

*Citation for published version (APA):*

Baltuška, A., Pshenichnikov, M. S., & Wiersma, D. A. (1998). SHG FROG characterization of . In *Technical Digest. Summaries of papers presented at the Conference on Lasers and Electro-Optics, 1998. CLEO 98* (pp. 461-462). University of Groningen, The Zernike Institute for Advanced Materials.

### Copyright

Other than for strictly personal use, it is not permitted to download or to forward/distribute the text or part of it without the consent of the author(s) and/or copyright holder(s), unless the work is under an open content license (like Creative Commons).

The publication may also be distributed here under the terms of Article 25fa of the Dutch Copyright Act, indicated by the "Taverne" license. More information can be found on the University of Groningen website: <https://www.rug.nl/library/open-access/self-archiving-pure/taverne-amendment>.

### Take-down policy

If you believe that this document breaches copyright please contact us providing details, and we will remove access to the work immediately and investigate your claim.

*Downloaded from the University of Groningen/UMCG research database (Pure): <http://www.rug.nl/research/portal>. For technical reasons the number of authors shown on this cover page is limited to 10 maximum.*

lated toward higher intensities by a simple increase in the frequency  $F$  of the applied voltage. This effect can be explained by the increase in the BSO admittance and the subsequent reduction in the voltage transferred to the liquid-crystal layer when  $F$  increases.<sup>1</sup> Thus, for  $F = 100$  Hz, a gain of 10 is obtained for  $I_0 = 1.2$  mW/cm<sup>2</sup> ( $V_0 = 9$  V) and for  $F = 400$  Hz, the same gain is observed for  $I_0 = 4$  mW/cm<sup>2</sup> ( $V_0 = 12.5$  V). These results show that the TWM gain can be optimized from submilliwatts to 10-mW intensities.

The influence of the other parameters, such as the grating period and the beam ratio, are also analyzed. Finally, image amplification is demonstrated.

In conclusion, we demonstrate amplification of a laser beam via two-wave mixing in a BSO liquid-crystal light valve with very low input intensities. Since LCLV can be designed for various ranges of wavelengths, it is also expected that this effect may be observed in spectral regimes not easily accessible by current nonlinear materials.

1. P. Aubourg, J.-P. Huignard, M. Hareng, R.A. Mullen, *Appl. Opt.* **21**, 3706 (1982).
2. D.M. Pepper, C.J. Gaeta, P.V. Mitchell, in *Spatial Light Modulator Technology*, U. Efron, ed. (Marcel Dekker, New York, 1995), chapt. 14.
3. V. Kondilenko, V. Markov, S. Odoulov, Soskin M., *Opt. Acta* **26**, 239 (1979).
4. I.C. Khoo, *IEEE J. Quantum Electron.* **32**, 525 (1996).
5. S. Bartkiewicz, A. Miniewicz, *Adv. Mater. Opt. Electron.* **6**, 219 (1996).

**CThV6** **3:45 pm**

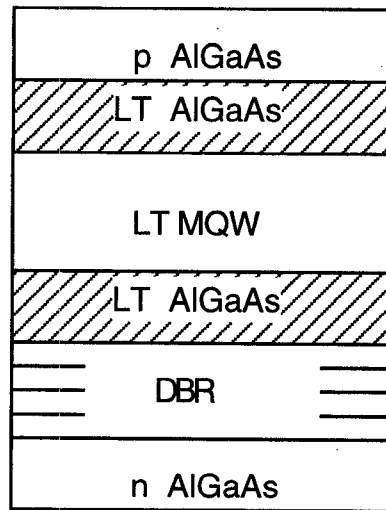
**Resolution limits of photorefractive MQW devices**

Akhelesh Abeeluck, Ergun Canoglu,\*  
Elsa Garmire, Parviz Tayebati,\*  
Robert N. Sacks,\*\* *Thayer School of Engineering, Dartmouth College, Hanover, New Hampshire 03755*

Photorefractive multiple-quantum-well (MQW) devices, attractive for two-dimensional optical information processing systems, have shown poor resolution, mostly due to lateral drift.<sup>1,2</sup> Adding traps throughout the MQW layer improves the resolution.<sup>3</sup> This paper demonstrates that low-temperature (LT) grown quantum wells can reach the fundamental resolution limit, which we have theoretically derived. Furthermore, because traps reduce the diffraction efficiency by reducing longitudinal transport, we have also investigated geometries that utilize conductive MQW with several localized trapping layers. Typical devices, operating in reflection, have 5- $\mu$ m resolution and 0.1% diffraction efficiency.

The devices are based on a p-i-n structure grown on a Bragg reflector (Fig. 1), with an intrinsic layer that contains MQW sandwiched between LT Al<sub>0.3</sub>Ga<sub>0.7</sub>As cladding layers. The shallow GaAs MQW are 5 nm wide and have 4-nm-wide Al<sub>0.1</sub>Ga<sub>0.9</sub>As barriers. When the MQW region is LT grown (as in Fig. 1) at a temperature to ensure good trapping, no lateral transport is possible.

Theoretical analysis of the device resolution



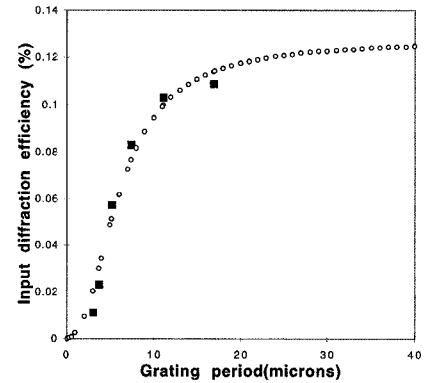
**CThV6 Fig. 1.** Geometry for reflective photorefractive MQW devices with LT grown intrinsic region consisting of MQW and cladding layers.

requires taking into account the effect of fringing on (1) lateral field, (2) longitudinal field, (3) field lines in the cladding region, (4) quadratic electro-optic effect, and (5) Bragg reflection. The analytic theory assumes a sinusoidal distribution of charge at the MQW-cladding interfaces, calculates the sinusoidal screening field and its effect on the complex refractive index, analyzes the optical-field distribution at the output face by accumulating localized phase contributions, and then calculates the far-field diffraction pattern. (Lateral carrier transport is neglected.) The result, in the Raman Nath approximation, shows that MQW of length  $d$  produces the following diffraction efficiency at grating period  $\Lambda$ :

$$\eta(\Lambda) = \eta_0 \frac{\left[ d + \frac{\Lambda}{2\pi} \sinh\left(\frac{2\pi d}{\Lambda}\right) \right]^2}{\left[ \cosh\left(\frac{\pi d}{\Lambda}\right) \left\{ 1 + \frac{\epsilon_1 \tanh\left(\frac{\pi d}{\Lambda}\right)}{\epsilon_2 \tanh\left(\frac{2\pi L}{\Lambda}\right)} \right\} \right]^4},$$

where  $L$  is the thickness of the clad layer, and  $\epsilon_1$  and  $\epsilon_2$  are dielectric constants of clad and MQW regions, respectively. Figure 2 shows the experimental input diffraction efficiency, along with a plot of the above equation, normalized at large grating spacing. Clearly, the analysis explains the experiment very well.

An alternative approach to increase diffraction efficiency is to use MQW grown at normal temperature (NT) and to localize the trapping by distributing several LT cladding layers within the intrinsic layer. These devices replace the LT MQW region by (1) a single NT MQW region, (2) three NT MQW regions separated by two additional LT cladding layers, and (3) five NT MQW regions separated by four additional LT cladding layers. The experimental resolution for these devices is somewhat poorer than the above theory predicts, a dis-



**CThV6 Fig. 2.** Experimental and theoretical results for input self-diffraction efficiency as a function of grating period.

crepancy that is presumably due to ignoring the lateral transport of carriers along lateral field lines within the NT MQW. The results of an analysis that includes lateral transport are presented and compared with the experiment. In addition, the dynamics of the distributed devices are discussed, determined by picosecond four-wave mixing experiments.

\*Coretek, Inc., 25B, Burlington, Massachusetts 01803

\*\*Department of Electrical Engineering, Ohio State, Columbus, Ohio

1. D.D. Nolte, *Opt. Commun.* **92**, 199 (1992).
2. E. Canoglu, C.M. Yang, E. Garmire, D. Mahgerefteh, A. Partovi, T.H. Chiu, G.J. Zydzik, *Appl. Phys. Lett.* **69**, 316 (1996).
3. I. Lahiri, K.M. Kwolek, D.D. Nolte, M.R. Melloch, *Appl. Phys. Lett.* **67**, 1408 (1995); I. Lahiri, M. Aguilar, D.D. Nolte, M.R. Melloch, *Appl. Phys. Lett.* **68**, 517 (1996).

**CThW** **4:30 pm–6:00 pm**  
Room 102

**Pulse Characterization Using Frequency-resolved Optical Gating**

Daniel J. Kane, *Southwest Sciences, Inc., President*

**CThW1 (Invited)** **4:30 pm**

**SHG FROG characterization of <5-fs pulses**

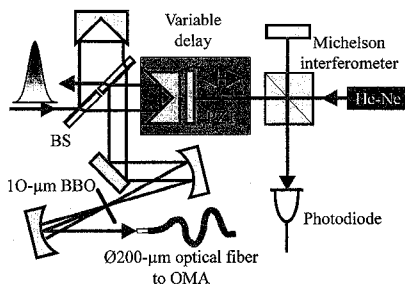
Andrius Baltuška, Maxim S. Pshenichnikov, Douwe A. Wiersma, *Ultrafast Laser and Spectroscopy Laboratory, Department of Chemistry, University of Groningen, Nijenborgh 4, 9747 AG Groningen, The Netherlands*

Accurate phase and amplitude characterization is essential for many ultrashort-pulse applications. Particularly, for optical pulses with bandwidths of hundreds of nanometers that demand sophisticated spectral phase correction, the full pulse description becomes indispensable. Because autocorrelation measure-

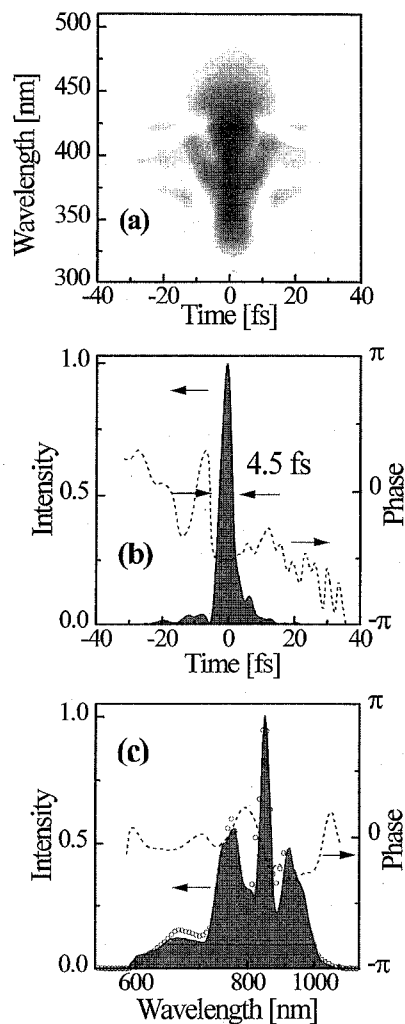
Thursday, May 7

ment allows only a rough estimate of pulse duration and does not reveal spectral structure, we adapted the second-harmonic generation frequency-resolved optical gating (SHG FROG) technique<sup>1</sup> to measure 15-nJ fiber-compressed pulses from our cavity-dumped Ti:sapphire laser.<sup>2</sup>

Because SHG FROG reproduces the geometry of a standard nonlinear optical experiment,



**CThW1** Fig. 1. Experimental setup for SHG FROG of 5-fs pulses. PZT: piezotranslation stage. BS: 50%, 0.5-mm-thick beam splitters.



**CThW1** Fig. 2. (a) Measured SHG FROG trace of compressed pulses. (b) Retrieved pulse shape (shaded) and temporal phase (dashed). (c) Fundamental spectrum measured with spectrometer (shaded) and retrieved by FROG (circles) and spectral phase (dashed).

this technique is ideal for characterization and on-target optimization of low-power ultrashort pulses that experience dispersive pulse broadening even from propagation through air.

In this paper, we demonstrate that even in the case of wide-bandwidth <5-fs pulses, true pulse parameters can be estimated on the FROG data correction<sup>3</sup> for the change in spectral sensitivity of the second-harmonic detector across the pulse spectrum and for the variation in frequency-doubling efficiency,<sup>4</sup> leading to a spectral filtering effect. We also investigate internal self-consistency checks<sup>3</sup> of our FROG data to validate the obtained results. Other subtleties of the measurement of pulses consisting of merely few optical cycles are discussed.

Our FROG apparatus is a convertible collinear/noncollinear autocorrelator designed for such extremely short pulses. This arrangement provides total symmetry and minimal phase distortion (Fig. 1). He-Ne laser interference fringes from a Michelson interferometer served as time calibration marks. The use of a piezotranslation stage ensured precise actuation of the optical delay. A 10- $\mu\text{m}$ -thick BBO SHG crystal was employed to maximize the usable phase-matching bandwidth. The recollimated second-harmonic beam was sent to a spectrometer via a  $\text{\O}200\text{-}\mu\text{m}$  optical fiber. Beam aperturing by the fiber allowed minimization of the effect of "temporal smearing,"<sup>3</sup> which otherwise, as estimated, would cause an  $\sim 10\%$  distortion in the pulse duration measurement.

The experimental SHG FROG is depicted in Fig. 2(a). The retrieved intensity and phase in the time and frequency domains are shown in Figs. 2(b) and (c), respectively. The obtained pulse duration is  $\sim 4.5$  fs FWHM, and variation of the spectral phase is less than  $\pm\pi/4$  across the whole bandwidth. These results fully confirm our previous analysis based on the interferometric autocorrelation.<sup>2</sup>

We also demonstrate application of SHG FROG in the measurement of strongly chirped white-light pulses. Whereas the basic limitations of the technique are imposed not by the pulse duration but by its bandwidth, additional effects, such as angular chirp of the background-free autocorrelation beam, should be considered in the case of chirped pulses.

1. K.W. DeLong, R. Trebino, J. Hunter, W.E. White, *J. Opt. Soc. Am. B* **11**, 2206 (1994).
2. A. Baltuška, Z. Wei, M.S. Pshenichnikov, D.A. Wiersma, *Appl. Phys. B* **65**, 175 (1997).
3. K.W. DeLong, D.N. Fittinghoff, R. Trebino, *IEEE J. Quantum Electron.* **32**, 1253 (1996).
4. A.M. Weiner, *IEEE J. Quantum Electron.* **19**, 1276 (1983).

#### **CThW2** **5:00 pm**

##### **Error bars in intensity and phase measurements of ultrashort laser pulses**

Michael Munroe, David H. Christensen, Rick Trebino,\* *National Institute of Standards and Technology, Optoelectronics Division, MS 815.04, 325 Broadway, Boulder, Colorado 80303*

How does one place error bars on a measurement of an ultrashort laser pulse? For many

years, the only available measure of an ultrashort laser pulse was the autocorrelation. Unfortunately, many quite different intensities correspond to the same measured autocorrelation, so even perfect measurement of the autocorrelation resulted in large, and unknown, error in the pulse intensity. Also, of course, no phase-versus-time information existed at all. As a result, it was not possible to retrieve a pulse intensity and phase. It made even less sense to attempt to place error bars on these quantities.

It is now possible to measure a pulse's intensity and phase versus time. The most commonly used method, frequency-resolved optical gating (FROG),<sup>1</sup> generates the full pulse intensity and phase versus time without making any assumptions about the pulse. As a result, it is potentially accurate, limited only by the accuracy of the measured trace.

Just how accurate is a given FROG measurement of a pulse? Some indication of the measured pulse accuracy is available from the FROG error—the rms difference between the measured and retrieved FROG traces. However, a method for determining the error in each of the retrieved intensity and phase points is needed. In other words, we need to be able to place error bars on the intensity and phase at each time (and frequency).

We present a simple, robust, and general method for doing this. We apply this method to both theoretical and experimental FROG measurements of pulses and show that it gives reasonable results.

We use the bootstrap method, which is a well-established statistical method.<sup>2</sup> In this case, it involves running the FROG algorithm several times for the measured FROG trace, but each time with a random set (about half) of the data points removed, and tabulating the statistics of the retrieved intensity and phase values obtained during these runs. It has been shown that, in general, the statistics of these resampled values approximate the actual statistics of the quantities of interest—in this case, the retrieved intensity and phase values at the various times (and frequencies).<sup>2</sup>

In this way, we can place error bars on the intensity and phase at each time or frequency. Figure 1 shows the retrieved intensity and phase of a theoretical Gaussian flat-phase pulse, with error bars determined this way. We added 1% uniform, additive noise to each point in the FROG trace to simulate experimental noise. The error bars represent the  $\pm 1$  standard deviation points of the mean value of each retrieved intensity or phase value for each time. Note that the resulting intensity errors are on the order of 1% of the intensity peak but vary with intensity. The phase noise is large in the pulse wings, as expected, because the intensity goes to zero there. Note also that  $\sim 60\%$  of the actual points fall within the error range, which indicates that this procedure is reasonable.

Figure 2 shows the retrieved intensity and phase of an experimentally measured pulse using the transient-grating FROG method,<sup>1</sup> with error bars obtained using the bootstrap method. The experimental noise corresponded to a few percent multiplicative noise in the FROG trace. Note that the resulting errors are also a few percent but vary with intensity.